The Design and Development of an Integrated Multi-Functional Microwave Antenna Structure for Biological Applications

Chris P. Hancock, *Senior Member, IEEE*, Nuwan Dharmasiri, Malcolm White, and Andrew M. Goodman

***Abstract*—A new multi-functional microwave antenna structure for use in biological applications in described. The antenna structure allows efficient propagation of Ku-band energy into biological tissue to perform *in situ* tissue characterization (measurement) and ablation or coagulation (treatment) of solid cancerous tumors and surrounding tissue. A calibration method that allows tissue characterization has been developed. The structure also supports a separate channel to allow material to be transported inside the structure without affecting the electromagnetic field propagation within the structure and the radiation pattern produced at the distal end. The structure is rigid and of small enough diameter to enable it to be introduced percutaneously into the human body under local anaesthesia.**

***Index Terms*—Brachytherapy, coagulation, conductivity, dielectric properties, false negatives, measurement of biological tissue properties, microwave ablation, multi-functional microwave antenna, needle biopsies, percutaneous insertion, relative permittivity.**

I. Introduction

THIS PAPER describes the design and development of a multi-functional near-field antenna that meets the challenge of matching the impedance of a rigid 2.2-mm diameter coaxial transmission line to the impedance of cancerous tissue, enables *in situ* tissue type/state measurements to be made, and allows biopsy samples to be extracted from (or material to be introduced into) the body, all in a single structure. The antenna structure supports the propagation of microwave energy at 14.5 GHz and so it is important to match the impedance of the structure to the impedance of the cancerous tissue in order to minimize losses and heating within the structure when full power (up to 50 W at the distal end) is being delivered into tissue.

Manuscript received October 15, 2012; revised March 15, 2013; accepted March 19, 2013. Date of publication April 04, 2013; date of current version May 02, 2013.

C. P. Hancock is with the Medical Microwave Systems Research Group, The School of Electronic Engineering, Bangor University, Bangor, Gwynedd LL57 1UT, U.K. (e-mail: c.hancock@bangor.ac.uk).

N. Dharmasiri is with Creo Medical Limited, Bath BA3 4QF, U.K. (e-mail: nuwan@creomedical.com).

M. White is with Creo Medical Limited, Chepstow NP16 5UH, U.K. (e-mail: Malcolm.White@creomedical.com).

A. M. Goodman is with the School of Electronic Engineering, Bangor University, Bangor, Gwynedd LL57 1UT, U.K. (e-mail: andy.goodman@bangor.ac.uk).

Color versions of one or more of the figures in this paper are available online at http://ieeexplore.ieee.org.

Digital Object Identifier 10.1109/TMTT.2013.2255620

Clinically, it is necessary for the antenna to produce spherical lesions of up to 4 cm in diameter, where the temperature needs to be elevated to a high enough value to cause cell death (or protein denaturization) throughout the volume, but not so high as to boil the tissue, e.g., the optimal range is between 45 °C–60 ° C. For a 4-cm lesion, the diameter of the tumor would be around 3 cm, with a 5-mm safe margin. For tissue type/state measurement, lower power (10 mW or less) is used and so it does not matter how much of this energy is dissipated within the antenna structure. The multi-functional antenna structure also meets the challenge of introducing a biopsy tube (or needle) into the antenna, which involves developing a means of passing the fluid (or material) from the inner conductor to the outside of the coaxial structure, without causing loss of function in terms of treatment and measurement capability.

No other single integrated antenna structure exists that is capable of making *in situ* tissue property measurements, taking tissue biopsies (or introducing material into the body at a specific location), ablating and/or coagulating a needle tract to prevent seeding, and ablating cancerous tumors. A system that uses a number of separate instruments for coagulating the needle tract, taking a tissue biopsy, and ablating tumors is described in [1], but the use of multiple instruments complicates the clinical procedure and does not allow *in situ* tissue type/state measurements to be made. Due to the need to use a separate tube, known as an introducer, to insert the various biopsy and ablation instruments into the body, the outside diameter (OD) of the device described in [1] is much larger than the multi-functional antenna described in this paper, i.e., 8–10-mm OD compared to 2.2-mm OD.

An overview of microwave antenna structures that have been developed specifically for tissue ablation or coagulation to treat clinical conditions, such as snoring, cardiac arrhythmias, benign prostatic hypertrophy, and liver ablation, using low-frequency microwave energy, i.e., 2.45 GHz or 915 MHz, is provided in [2]–[10]. These antenna structures can only be operated in treatment mode. A range of coaxial antenna structures developed to characterize biological and non-biological materials over a band of frequencies between 50 MHz–20 GHz are also considered in [11]–[17]. These antenna structures have been developed to be operated in measurement mode only.

It has been shown that high-frequency microwave energy in the Ku-band can be used to produce fast and controlled ablation of biological tissue [18]. The effectiveness of using energy at 14.5 GHz for coagulating blood by overcoming the "heatsinking" effect caused by blood flow, which is of particular significance when considering the treatment of tumors due to their inherent vascularity, has also been demonstrated.[1] Furthermore, it has also been documented that lower frequency microwave energy in the ultrahigh-frequency (UHF) band offers advantage over lower frequency RF energy for ablation of tumors within solid organs [19]–[21], although there are still drawbacks in terms of not being able to cope with high perfusion, lack of control of depth of coagulation, and limited measurement resolution. The new multi-functional antenna structure described in this paper overcomes these issues.

The new near-field multi-functional antenna structure described here is unique in that it provides the following functions using one single structure:

1) removal of tissue samples for biopsy;
2) introduction of materials into the body;
3) ablation/coagulation of needle track;
4) measurement of the dielectric properties of biological tissue (healthy tissue, cancerous tissue);
5) location of boundary between two types of tissue (location of center of tumor);
6) *in-situ* ablation of tumor if biopsy results are positive.

The ability to produce controllable and focused ablation and coagulation of biological tissue enables a uniform channel of ablation to be created as the antenna is removed from the body. In this instance, the diameter of the ablation is larger than the OD of the antenna shaft, i.e., a channel with a 4-mm diameter may be created for the antenna with a 2.2-mm OD described in this paper. This feature ensures that any cancerous cells present at the radiating tip of the antenna cannot be reintroduced back into healthy tissue structures between the surface of the skin and the cancerous site when the antenna is removed from the body, which is a situation that has been identified as a risk to patients who have undergone fine needle aspiration cytology [22]. The ability of the new antenna described here to produce spherical lesions in a fast and controllable manner, i.e., a 20-mm-diameter spherical lesion in 2 min, enables the tumor to be ablated *in situ* using the same structure introduced along the same channel if the biopsy results turn out to be positive. Furthermore, the ability to use the same antenna structure to measure the dielectric properties of biological tissue enables various biological tissue structures in contact with the radiating section of the antenna to be identified. In this work, it is shown that boundaries between two adjacent tissue structures can be identified using the multi-functional antenna structure, which provides a number of useful clinical advantages; one of which is to enable the distal end of the radiating section of the antenna to be positioned at the center of a spherical tumor to reduce the risk of taking a biopsy sample that gives a false negative result—a situation that is most undesirable since it necessitates the need to repeat the procedure several times, i.e., in fine needle aspiration [23] where multiple insertions may be made to extract fluid from a cyst or cells from a solid lesion. The ability to position the radiating section of the antenna at the center of the tumor also helps ensure that complete ablation of spherical tumors is carried out and that a uniform zone of healthy tissue is destroyed around the tumor to provide a safe margin, i.e., a safe margin of 5 mm may be provided for a 10-mm-diameter tumor, thus the overall diameter of ablated tissue would be 20 mm. The ability to accurately measure properties of tissue in contact with the radiating section of the multi-functional antenna structure also allows materials to be introduced into the body in precise manner. An example of this is in brachytherapy, involving the precise placement of sources of radiation at the site of the cancerous tumor; this offers significant benefit over the main alternative, in which high-energy X-rays are directed into the body from the outside. The probability of placing the radioactive seed into the center of the tumor using the multi-functional antenna structure would be significantly increased due to the ability of the device to identify an interface between two tissue types. Again, the ability of the multi-functional antenna to coagulate and/or ablate the entry channel to prevent seeding is advantageous in this application. The physical requirements relating to the antenna structure and the ablation profile produced were discussed with two leading U.K. surgical oncologists specializing in the treatment of breast tumors, and these requirements are captured in a user requirements document [40] for a new breast cancer treatment system.

[1]Hancock *et al.*, pre-clinical work carried out on *in-vivo* porcine and rat liver models between 2005–2009 using the microblate cancer treatment system and other systems developed by MicroOncology Ltd. and Creo Medical Limited (protocols and details of this work are company confidential).

II. Overall System Incorporating Antenna

The complete system, which includes a vector reflectometer measurement circuit to enable *in situ* tissue property measurements to be made, a dynamic impedance matching system to deliver a controlled pulses of energy into tissue to ensure repeatable ablation volumes are produced, and the tissue/material biopsy/introduction feature, is shown in the block diagram given in Fig. 1, where the emphasis is on the multi-functional antenna. A more detailed overview of the overall system can be found in [24].

From Fig. 1, the dynamic matching feature comprises: a high-power transmitter capable of producing power in the Ku band of up to 50-dBm (100 W) continuous wave (CW), a matching network for tuning, a tuning element adjuster, a waveguide switch (to switch between measurement and treatment modes), a low-loss microwave cable assembly, the multi-functional antenna, a double heterodyne receiver, and a microcontroller. The heterodyne receiver enables phase and magnitude information relating to the biological tissue in contact with the radiating tip of the antenna to be extracted; this information is used to adjust the tuning elements to match the microwave source with the changing impedance of the tissue for maximum power transfer. It must be ensured that the insertion loss of the microwave cable and the antenna is as low as possible in order to prevent loss of energy in a standing wave in the "cavity" between the tuning network and the radiating tip of the antenna; a detailed description of the dynamic impedance-matching system is given in [25]–[28]. The low-power integrated tissue measurement system operates at 10-dBm (10 mW) CW, and has in addition, a bandpass filter to remove any components of the first local oscillator (transmitter signal is at 14.5 GHz and first local oscillator signal is at 14.45 GHz), a directional coupler to sample the forward signal for carrier cancellation and to compensate for measurement drift (full details on methods of drift compensation is given

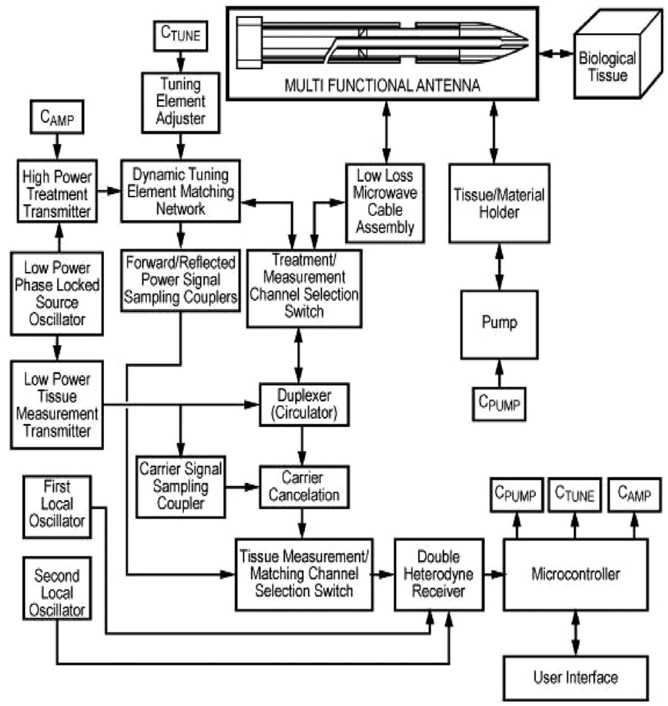

Fig. 1. Overall system diagram showing tissue detection, matched ablation, and biopsy/material removal/introduction features.

in [29]–[31]), a duplexer to direct the measurement signal to the biological tissue and to receive the returned signal once the antenna has made contact with this tissue, a waveguide switch, a carrier cancellation circuit [to cancel out forward breakthrough signal from the first port to the third port of the circulator (duplexer)], a double heterodyne receiver, and a microcontroller. The phase and magnitude information is used to provide information concerning the tissue type/state. In order to be able to make valid tissue measurements, the multifunctional antenna is calibrated using three fluid loads that each provide reproducible impedances and enables the complete radiating section of the antenna to make contact with the calibration load. Full details of the method used to calibrate the antenna can be found in [27] and [28].

The multi-functional antenna described here has been used with the system shown in Fig. 1 to effectively demonstrate controlled tissue ablation and the ability to distinguish between healthy and cancerous tissue.

In order to prevent high voltages and/or currents building up in the resonant cavity between the tuner and the radiating tip, the multi-functional antenna has been designed to be impedance matched to the initial impedance of a representative tumor model [27], [28].

III. Antenna Design and Fabrication

The first phase of the design was based around a small diameter antenna structure for near-field propagation into biological tissue that could be used to perform tissue ablation and measurement only. The second phase included the design of an integrated hollow channel to remove material from, or introduce material into, the body.

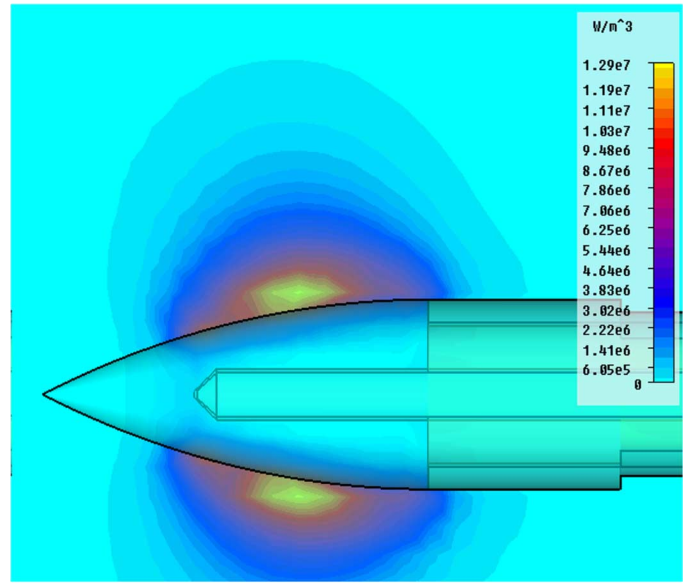

Fig. 2. EM field simulation for antenna without hollow center conductor showing power density in tumor model.

A. Ablation and Measurement Only

The structure is to be inserted percutaneously into the body and cause a minimal amount of scarring. Therefore, the OD should be as small as possible, i.e., not exceed 2.2 mm. The structure is also required to have a smooth sharp point for ease of insertion, and produce a beam of radiation that results in a spherical heating pattern reaching the tip of the radiator, and out to between 10–15-mm radius. It was initially considered how a conical beam might be launched, using an assembly of two swept dipoles in a "turnstile antenna" like arrangement, to generate a circularly polarized conical beam. However, due to the complexities of the feed structure for such an arrangement, it would be impossible to fit this inside the 2.2-mm-diameter cylinder, especially when the maximum power level of 50-W CW is being generated at the radiating tip of the structure. After some trial and error, it was found that a "monopole" antenna in a high dielectric sheath would give the desired power absorption pattern in tumor.

The power absorption simulation in a "dummy" tumor for the final design is shown in Fig. 2, where it can be seen that the power density is at its peak value near the tip of the inner conductor. The highest value is 1.4×10^7 W/m^3, for an input power of 1 W.

It can also be seen that the heating near the end of the outer sheath is less than at the tip of the inner conductor, and power flow back down the outside of the cable is minimal. The lower absorption near the tip is potentially a problem, but it was found in practical testing that due to the small volume of this region, thermal conduction (not included in the simulation) raised the temperature in the this region adequately. The absence of any power flow down the outside of the cable is an important factor as it prevents the ablation profile wrapping back along the cable and it also means that it is not necessary to include a separate choke in the design, which would be difficult given the constraints on the overall diameter. It is also required that the antenna is mismatched when propagating into free space (or air). As the impedance of free space differs significantly from that of

TABLE I
CHARACTERISTICS OF LOW-LOSS RIGID MICROWAVE CABLE ASSEMBLY SUITABLE FOR ANTENNA

Parameter	Value/Material
Inner conductor material	Silver plated solid Copper-clad Steel
Outer Diameter (mm)	0.51 ± 0.01
Dielectric material	PTFE
Outer Diameter (mm)	1.67 ± 0.02
Outer Conductor material	Stainless steel/Copper
Outer Diameter (mm)	2.20 ± 0.02
Dielectric constant (ε_r)	2.04
Attenuation (dB/100m) at 10GHz	217
Impedance (Ω)	50 ± 1.0
Cut off frequency (GHz)	60

fat or tumor, it was found that little optimization was required to obtain this condition. Thus, the structure will not efficiently radiate 14.5-GHz energy into free space. This aspect is important due to potential safety and interference issues.

Simulation results for the structure show significant differences between the magnitudes and phases of the reflections from the antenna when placed in air, in fat and in "dummy" tumor. This indicates that the material around the antenna can be identified by measurement of the amplitude and phase of the reflected signal, which is the second aspect of the antenna design. The geometry of the optimized ablation and treatment antenna that captures the findings obtained from the electromagnetic (EM) modeling work and the practical constraints is given in [34] and [35]. The near-field antenna structures considered in this work were designed and simulated using Computer Simulation Technology (CST) Microwave Studio. All models were built assuming fourfold symmetry in order to minimize run times and to keep the models as small as possible. This was found to be necessary due to the tumor and ceramic requiring a large number of mesh points. Therefore, the antenna structure and the tumor were modeled as one-quarter of a cylinder with magnetic walls on the two straight sides. The signal is strongly attenuated in tissue, so only a relatively small volume of tissue was needed, to be big enough that no distortion of the power absorption profiles could be discerned for the lowest loss tissue, which was fat.

The model was built using the dimensions of low loss 50-Ω semi-rigid cable with a low-density PTFE dielectric separating the inner and outer conductors. The center conductor was of diameter 0.508 mm. The sheath was of inner diameter 1.544 mm and of outer diameter 2.16 mm. The outer jacket was made from stainless steel in order to provide the necessary rigidity required to enable the surgeon to introduce the antenna directly into patient tissue without the need to use an introducer, and also for biocompatibility. The mechanical and electrical characteristics of the most appropriate coaxial structure are given in Table I. In order to ensure the insertion loss at the frequency of choice, 14.5 GHz, was low enough to prevent the cable heating and also to limit the operation of the resonant tuning cavity, it was necessary for the inside of the stainless steel outer jacket to be silver plated.

The PTFE insulator was removed from the end of the coaxial structure for a distance of 7 mm, and an alumina cylinder of the same inner and outer diameter substituted. At the outer end, the alumina cylinder has a step out to the outer diameter of the coaxial structure (the sheath), and then an ogival taper to a point over 5 mm. The inner of the coaxial structure extended out 3 mm past the end of the sheath, into a hole in the ceramic tip.

TABLE II
CHARACTERISTICS OF LOW-LOSS MICROWAVE CERAMIC SUITABLE FOR IMPEDANCE TRANSFORMER AND RADIATOR

Parameter	Value/Material
Dielectric constant (ε_r)	9.0
Dissipation factor (tan∂) at 10GHz	0.00045
Maximum temperature (°C)	1800
Thermal expansion coeff. (x10^{-6}/ °C)	8.4

A 7-mm-long ceramic cylinder is a three-quarter wave impedance transformer, and matches the 50-Ω impedance of the coaxial structure to the impedance of the antenna buried in the tumor model, which is close to 7 Ω. The geometry was optimized to give a good impedance match to a "dummy" tumor model, with a dielectric constant 40 and loss tangent 0.5 at 14.5 GHz [36]. It was found that the length of the cylinder could be adjusted to match other tissue types. Models for fat and liver at 14.5 GHz, obtained from data provided in [37], were also considered. An ogoval tip was chosen as compromise between a shallow taper, which had the effect of diffracting the radiation from the antenna slightly in the forward direction, but resulted in a weak tip, and a rapid taper, which produced a stronger tip, but resulted in an unacceptable split-lobe pattern.

The design of the integrated impedance transformer and near-field radiator used a microwave ceramic material known as Dynallox 100 (from Dynamic Ceramic Ltd.). The important electrical and mechanical properties associated with this material are given in Table II.

In order to retain and fasten the ceramic tip in the coaxial cable, a groove was formed in the body of the ceramic and held by constricting the outer conductor of the coaxial cable assembly to produce a cylindrical depression (crimp) into the groove. It was found that the position and size of the groove and crimp could be optimized to improve the match into tumor.

Two alternative methods considered to achieve this function involved the use of plastic or metal retaining pins, inserted through the outer conductor of the coaxial structure and the body of the ceramic, but, in practice, it was found to be difficult to make the pins large enough without making the holes in the ceramic so large as to seriously weaken the structure, whereas cylinders with a cylindrical groove have proven to be robust.

It was found that if the ceramic tip and the PTFE dielectric of the coaxial cable were designed to meet exactly, the presence of a small air gap made a significant difference to the impedance match of the antenna into tissue. Due to the difficulty of obtaining an exact fit without an air gap between the ceramic and the PTFE, a deliberate conical air gap was designed in. The performance of the final antenna design was not found to be dependent on the exact size of this air gap, i.e., a gap of up to $+/-0.25$ mm does not affect the impedance match.

A photograph of the antenna and the ceramic tip/transformer is given in Fig. 3.

B. Inclusion of Center Channel and Feed/Extraction Pipes

The skin depth at 14.5 GHz in copper and silver is 0.549 and 0.533 μm, respectively, which implies that the EM field is

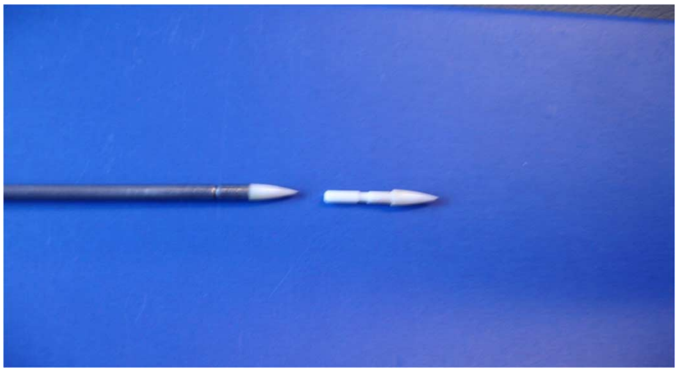

Fig. 3. Photograph of distal end of antenna and ceramic tip/transformer.

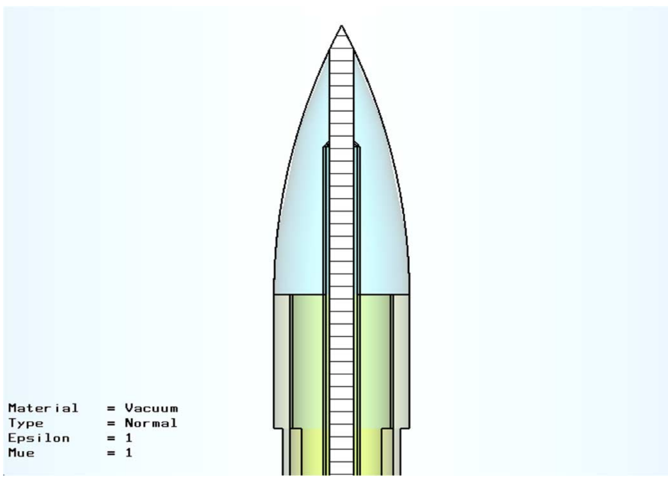

Fig. 4. Cross-section of antenna with hollow channel for material transport.

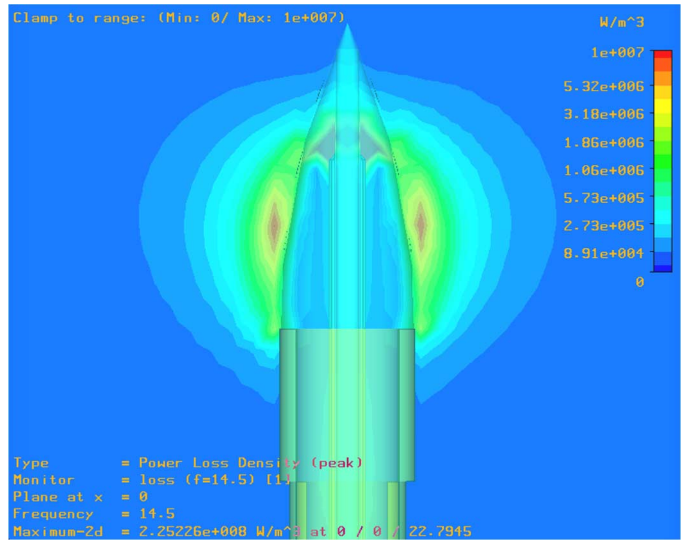

Fig. 5. Power loss density in tumor model with hollow channel.

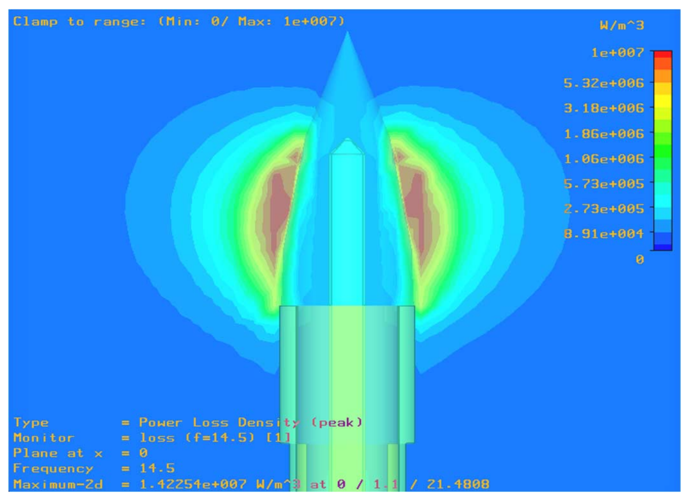

Fig. 6. Power loss density in tumor model with no biopsy channel.

still able to propagate along the structure with a hollow center conductor. This hollow center conductor may be used to deliver or extract material from the site where the tip of the radiating antenna is located. A 0.4-mm diameter tube can be incorporated down the center of the inner conductor of the antenna, extending out through the ceramic tip. A biopsy tube was modeled running down the axis of the center conductor of the coaxial line, and through the end of the ceramic tip. In the models produced for this work, the tube extended from 2 mm from the input port to the end of the ceramic tip, which was located a distance of 25 mm from the input port. The entire biopsy tube was modeled in every case as being full of a material that may, in practice, surround the radiating tip, i.e., tumor, breast fat or air. A cross section of the antenna with the biopsy channel is shown in Fig. 4, where the biopsy channel is shown with horizontal hatching.

Because of the fourfold symmetry used in the modeling, when the model included the tubes to transfer material, there were four tubes leading from the center biopsy channel to the outside of the structure.

In each case, the presence of the biopsy sample in the tip of the antenna was found to modify the match to the antenna. The presence of the biopsy sample inside the center conductor had no effect on the microwave performance of the antenna, except for the first millimeter from the tip. This is because the walls of the center-conductor tube are more than several skin depths thick so that the biopsy sample is shielded from fields outside the center conductor, and the biopsy tube is well below cutoff for propagation of waves down the tube, even taking into account that the biopsy sample may have a very high dielectric constant. For a dielectric constant of 50, which is the highest likely to be found in envisaged uses, the tube would need to have an internal diameter of 3.5 mm or more for propagation to take place, and even in this instance, the high losses in the sample would result in very rapid attenuation of the signal along the first few millimeters of the tube. Fig. 5 shows the power loss in a structure comprising the antenna containing tissue biopsy material and surrounding tumor. It can be seen that there is very little loss in the biopsy material. For direct comparison, Fig. 6 shows the power loss for the antenna without a biopsy tube.

It can be seen that the presence of the biopsy sample results in more power absorption near the tip of the antenna. There is also a slight lowering of the peak absorption.

This is due to two effects; the first is that when there is a biopsy tube present, the power is spread over a larger volume, as there is more power absorbed near the tip, and secondly, the biopsy worsens the match of the antenna, so less total power is

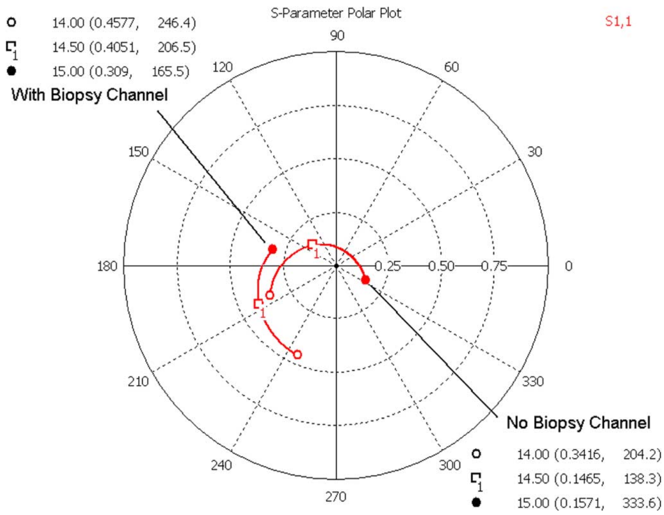

Fig. 7. Impedance match with and without biopsy channel.

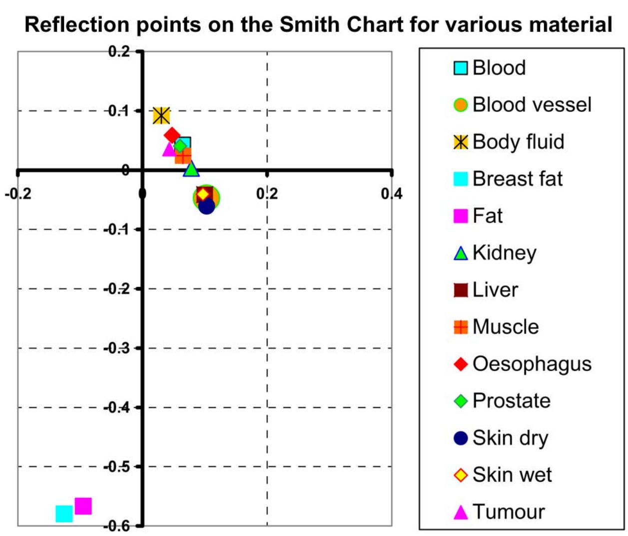

Fig. 8. Predicted range of impedance matches into various tissue types.

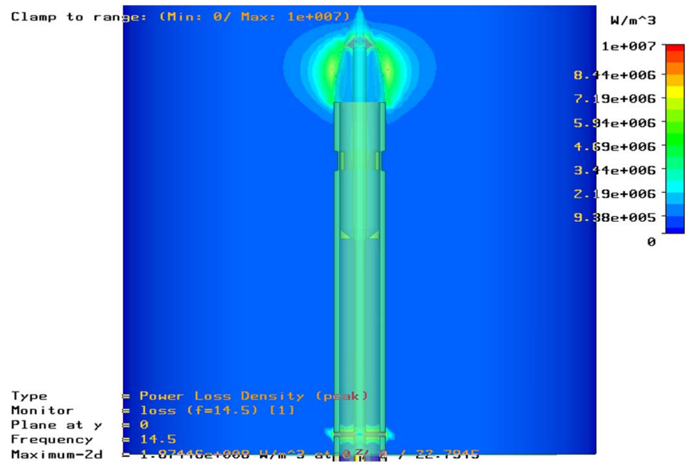

Fig. 9. Power loss density in biopsy antenna with pairs of feed-though holes.

delivered. The dynamic tuning mechanism that forms a part of the overall system will recover most of the loss due to the second effect as this mismatch will be automatically compensated for. The change in the power absorption pattern near the tip when the biopsy tube is introduced may also be advantageous as it will result in more heating occurring near the tip.

The change in impedance match introduced by the biopsy channel at the radiating tip of the antenna is illustrated in Fig. 7. The match is shown for a range of frequencies between 14–15 GHz, with a marker at 14.5 GHz.

It can be seen that there has been a significant shift in the match, i.e., about 80° rotation and a change from 17- to 8-dB return loss. In order to take this into account in the overall system, it is necessary to re-calibrate the system since the magnitude of the shift is larger than the range of impedances reported for different blood-rich tissues using the unmodified antenna. This range is shown in Fig. 8. The cluster of points toward the top of Fig. 8 is for blood-rich tissue, the two points at the bottom are for fatty tissue.

In order to remove the biopsy sample from the contact tissue, a connection to the hollow channel within the center conductor is required. This connection must pass through the wall of the coaxial assembly. The tubes transport the biopsy sample contained inside the inner conductor channel to the outside of the outer conductor. The tubes connect to the wall of the inner conductor, pass through the PTFE dielectric, and protrude through the wall of the outer conductor.

A number of designs using 0.2-mm-diameter tubes were modeled to establish the optimal connection points and the number of tubes required. Four 0.2-mm tubes were considered optimal because the total cross section then equals the cross section of the biopsy channel through the tip of the antenna. The total cross section of the biopsy channel is a compromise between minimizing the constriction of flow of the biopsy sample, and leaving sufficient width of wall on the inner conductor, between tubes, for good microwave conduction, and strength. A ring of tubes near the proximal feed end of the antenna was modeled.

The biopsy sample is gathered from the four holes in the outer conductor of the coaxial line by an exterior sleeve. It was found that the introduction of the four tubes containing tumor samples taken from the biopsy reduced the power delivered to the tumor, as can be seen by the "greening" of the area around the antenna tip shown in Fig. 9. The power loss density in the whole antenna is shown in Fig. 9, and a magnified picture of the fields at the location of the tubes is shown in Fig. 10, which confirms there is significant power loss density in and around the tubes.

The arrangement of the holes between the inner and outer conductors was modified in order to try to reduce the mismatch and/or loss caused by the holes. Instead of placing the four holes the same distance from the antenna, at 90° spacing around the axis, they were arranged as two in-line pairs, spaced 180° around the axis. To do this, the symmetry of the model had to be reduced, from fourfold to twofold, resulting in longer run times.

A quarter-wavelength separation of 3.5 mm was first tested since this is the ideal separation to give cancellation of two simple identical lossless mismatches. The quarter-wavelength

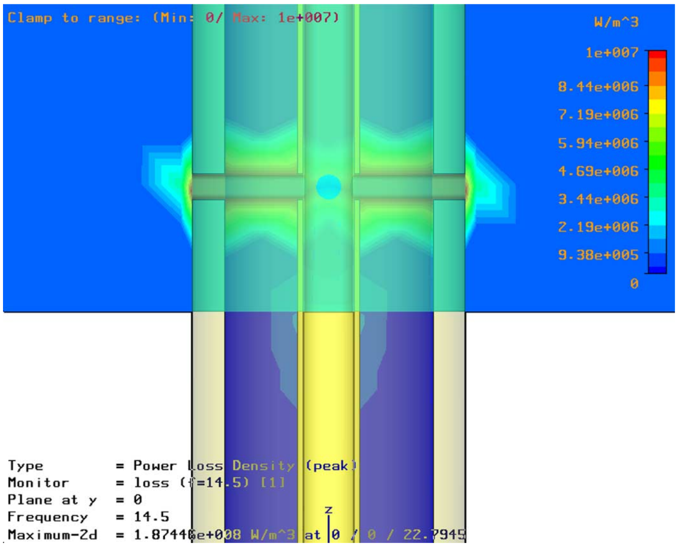

Fig. 10. Detail of loss density around the four tubes.

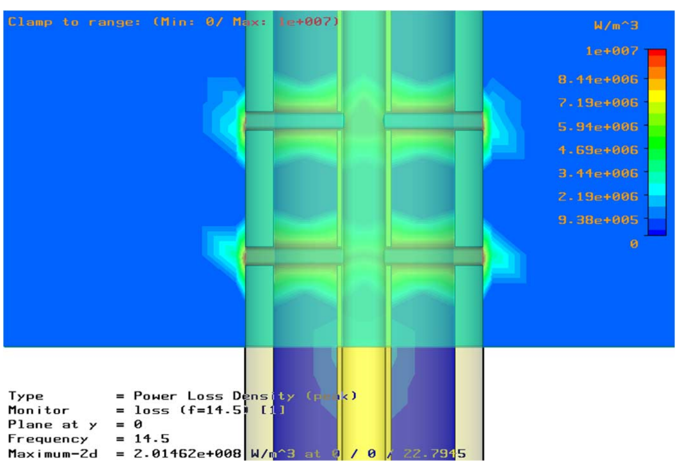

Fig. 11. Loss density for four holes with 1.5-mm spacing between pairs.

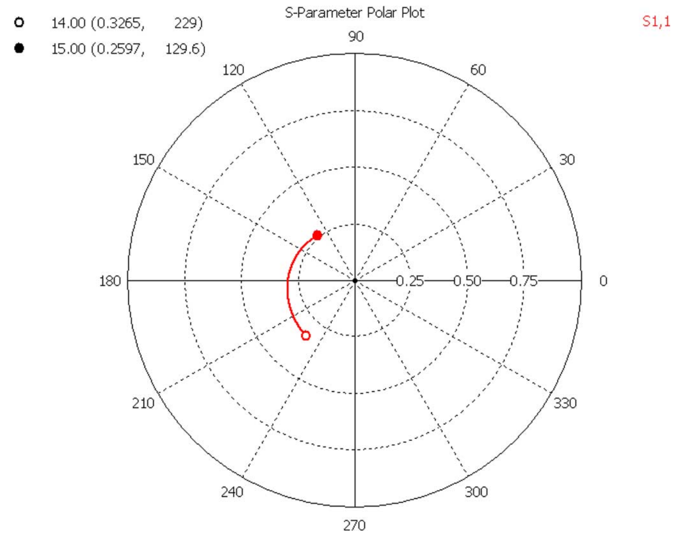

Fig. 12. Match for four holes with 1.5-mm spacing between pairs.

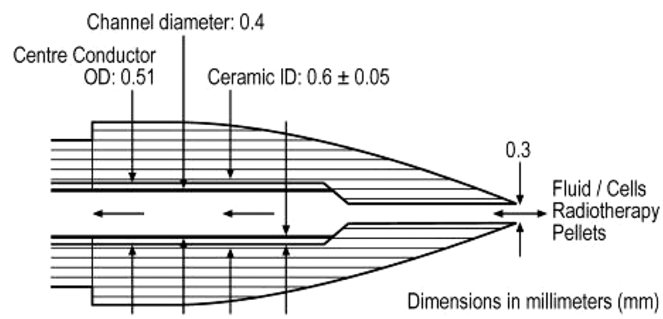

Fig. 13. Close-up of the design of the radiating tip that includes the channel used to transport biological tissue or introduce radioactive pellets.

separation was shown to give no improvement so the separation was reduced to 2 mm and then to 1.5 mm. The power loss density around the holes and the impedance match are show in Figs. 11 and 12. Although Fig. 11 indicates there is no apparent reduction in the loss density around the holes, it is clear from Fig. 12 that the mismatch has been reduced, which results in an overall improvement in performance compared to having all four holes at the same distance from the radiating tip of the antenna. This structure has not yet been fully optimized, for instance, metallizing the walls of the holes is a modification that might give improved performance.

From these simulations, it has been shown that the antenna may be modified to introduce a biopsy channel with a diameter of 0.4 mm, with either a ceramic or a metal tube, and with an appropriate material feed/extraction arrangement, without significantly degrading the overall electrical performance of the treatment/measurement antenna.

The final geometry of the distal end of the multi-functional antenna is shown in Fig. 13. This is also captured in [36] and [37].

IV. Results

A. Tissue Ablations

To demonstrate the effectiveness of the antenna in terms of performing tissue ablation, blocks of porcine liver were prepared from a complete *in vitro* liver. The size of each block was approximately: 5 cm (wide) × 2.8 cm (deep) × 3.5 cm (high). The testing was carried out at room temperature. The antenna was inserted into the center of each block using a test jig designed and developed to enable the distal end of the radiating tip to be located at the same position inside the tissue block prior to the energy being delivered. All tissue ablations were performed using the same antenna structure. External microwave radiation was monitored at all times using an Nardalert XT, model number D8862.

For each ablation, 2000 J of energy was delivered using 50-W peak power (referenced to the distal radiating tip of the antenna). The duty cycle was 33% (1 s ON and 2 s OFF for a total duration of 120 s). A cross section through six representative ablations, produced using these settings, is shown in Fig. 14, and the measured width and depth of the ablations is given in Table III.

The standard deviation in depth is 0.91 mm and the standard deviation in width is 0.75 mm.

The sizes of ablations given here are representative of the sizes of tumors that would be treated using the antenna.

Fig. 14. 2000 J of energy delivered into six blocks of *in-vitro* porcine liver using the multi-functional antenna structure.

TABLE III
ABLATION SIZES PRODUCED IN MORBID PORCINE LIVER

Sample	Width (mm)	Depth (mm)
Block 1	20	19
Block 2	18	18
Block 3	20	20
Block 4	19	20
Block 5	20	20.5
Block 6	19	19
Mean value	19.33	19.42
Standard deviation	0.816	0.917

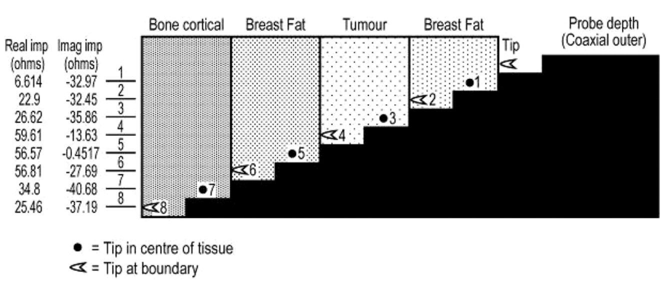

Fig. 15. Results from model using CST Microwave Studio showing changes in complex impedance with the tip of the antenna in bulk tissue and at the boundary between two adjacent tissues.

B. Tissue Measurements

1) Modeled Results: A model using representative tissue types associated with the structure of the human breast was created using CST microwave studio. The optimized antenna structure described above was used in the model and the change of impedance as the antenna was inserted in 5-mm steps through successive 10-mm-thick layers of breast fat, tumor, breast fat, and cortical bone was recorded. This model and the results obtained are shown in Fig. 15.

It can be seen that it is theoretically possible to identify the boundary between two adjacent tissue types as well as being able to identify a single tissue structure surrounding the radiating tip of the antenna. The plot of the locus of the reflection as the antenna is inserted in 5-mm steps from air through the

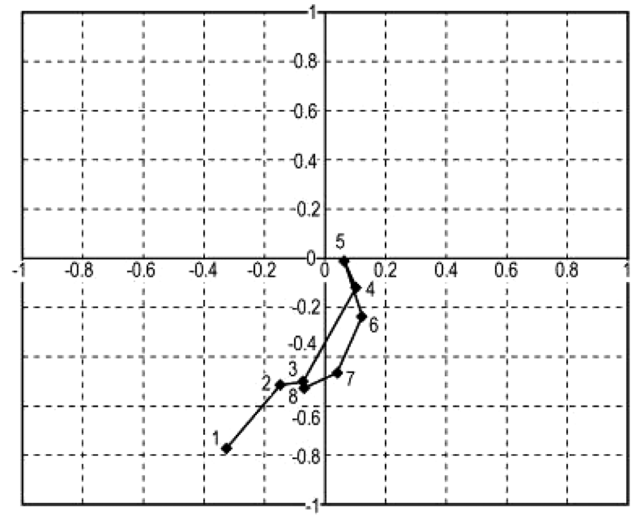

Fig. 16. Locus of radiating tip as it passes through layers of tissue.

10-mm-thick layers of fat, tumor, fat, and bone is also shown in Fig. 16.

2) Calibration and Measured Results: In order to perform meaningful tissue measurements using the multi-functional antenna, it was necessary to develop a specialized method of calibration since the radiating tip does not have a standard impedance of 50 Ω, and the shape does not allow conventional calibration loads to be connected. Also, in final use, the antenna must be sterile and the loads must be made from a biocompatible material. Therefore, performing a calibration using normal calibration standards and calibration method is not possible. A calibration technique involving liquid loads using miscible solutions was found to overcome these issues. The calibration process adopted here to validate the operation of the multi-functional antenna structures, operating in measurement mode, involved the antenna being directly connected to a calibrated Agilent 85131F 3.5-mm flexible test port cable and a 8720ET vector network analyzer set up to measure complex impedance at a spot frequency of 14.5 GHz. Each antenna was inserted into a glass test tube containing a 10-mL liquid load, made up of various concentrations of anhydrous ethanol and de-ionized water, to depth of more than 1 cm and held in the middle of the test tube using a rubber bung to prevent coupling of the microwave energy into the glass. A calibration was performed using the liquid calibration standards made up of miscible solutions of anhydrous ethanol and de-ionized water at room temperature. The following standards were used:

1) 100% de-ionized water;
2) 50% de-ionized water + 50% anhydrous ethanol;
3) 100% anhydrous ethanol.

Error corrected measurements were then conducted using a range of morbid tissue models to validate the tissue type recognition feature and also to demonstrate measurement repeatability.

Following calibration, the complex impedance of a variety of *in vitro* tissue models was measured using the multi-functional antenna. The material models were contained inside a transparent plastic holder that allowed a layered structure to

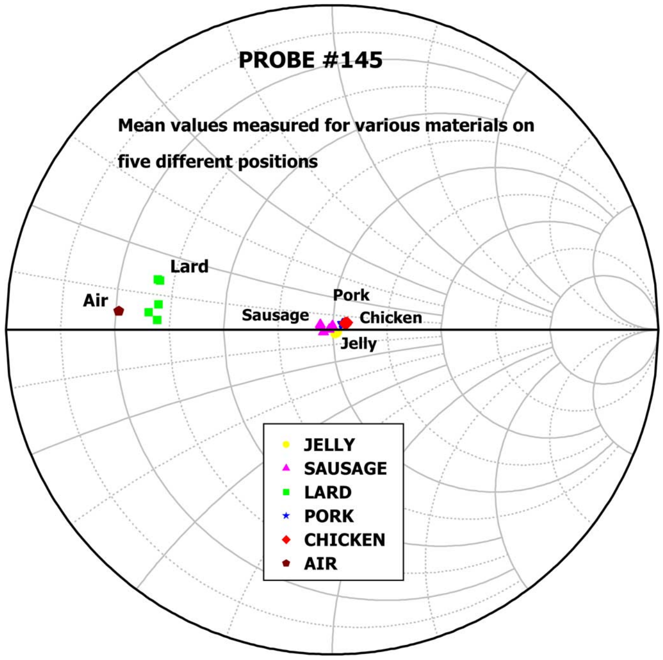

Fig. 17. Repeatability measurements of complex impedance made using a single multi-functional antenna inserted five times into a sandwich of heterogeneous tissue models.

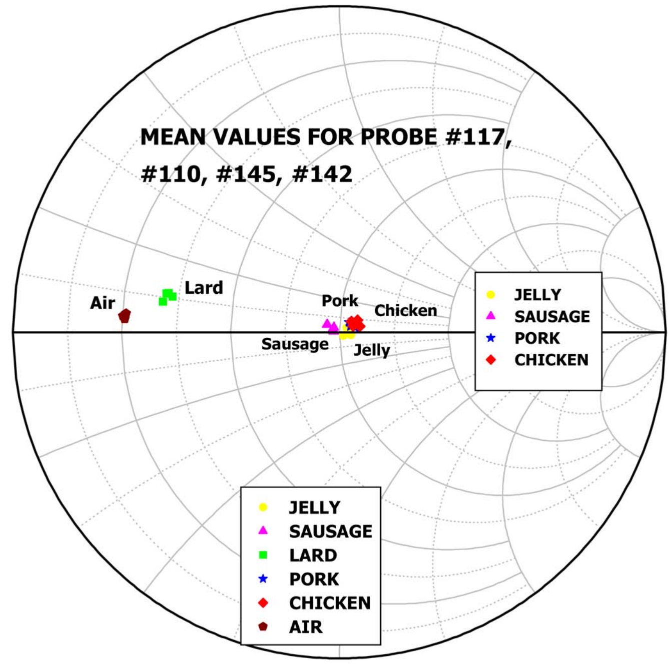

Fig. 18. Tissue type recognition measurements carried out using four separate multi-functional antenna structures with a full liquid calibration carried out prior to making the measurements.

TABLE IV
MEAN STANDARD DEVIATION FOR A SANDWICH OF HETEROGENEOUS TISSUE MODELS USING THE MULTI-FUNCTIONAL ANTENNA STRUCTURE

Tissue	Mean Standard Deviation	
	Real	Imag
Air	0.017	0.020
Jelly	0.33	0.21
Sausage meat	1.45	0.76
Lard	0.44	2.19
Pork	0.23	0.25
Chicken	0.30	0.26

TABLE V
MEAN STANDARD DEVIATION FOR THE HETEROGENEOUS TISSUE USING FOUR SEPARATE CALIBRATED MULTI-FUNCTIONAL ANTENNA STRUCTURES

Tissue	Mean Standard Deviation	
	Real	Imag
Air	0.14	0.27
Jelly	1.05	1.10
Sausage meat	0.94	0.87
Lard	0.50	0.56
Pork	1.01	0.89
Chicken	1.33	1.02

be constructed. Prior to placing the tissue layers inside the plastic box, a jelly-water solution was poured into the box. This solution was allowed to partially set before the tissue models were introduced. The jelly-water solution enabled the tissue models to bind together and allowed the heterogeneous tissue models to be suspended. The solidified jelly-water concentration also provided an additional material that could be used in the tissue recognition measurements. The radiating tips of the antennas were inserted repeatedly into the plurality of heterogeneous materials. The measured complex impedances for a single antenna (reference number 145) using the morbid tissue models described above, with full calibration performed prior to performing the measurements, is shown in Fig. 17. In order to demonstrate repeatability, the measurement was carried out five times. These measurements indicate that consistent values of complex impedances can be obtained when pushing the radiating tip of the antenna into the sandwich of heterogeneous tissue models. Table IV gives the mean standard deviation values for the real and imaginary parts of the measured complex impedances.

Finally, to demonstrate the ability to calibrate the non-standard multi-functional antenna structures using loads made from miscible solutions, four multi-functional antennas, randomly selected from a batch of 150 units built for pre-clinical and pilot clinical testing, were calibrated and then measured. Fig. 18 shows the overall mean measured values of complex impedance for the heterogeneous tissue. Table V gives the mean standard deviation values of the real and imaginary parts of the measured complex impedances.

These measurements indicate that the multi-functional antenna structures developed in this work can be used to make repeatable measurements on a range of materials that exhibit a wide dynamic range of complex impedance values.

V. DISCUSSION AND CONCLUSION

This paper has described the design and development of a new small geometry multi-functional antenna for high- and low-power near-field propagation into biological tissue for tumor/needle track ablation, and for tissue type/state measurement, respectively. The antenna structure also contains a hollow channel with an arrangement of feed tubes to enable tissue biopsies to be taken or for radioactive material to be introduced into the body for applications involving extremely localized radiotherapy. The ceramic radiator that forms an integral part of the antenna structure was optimized using EM field modeling tools to accommodate this feature. The final design meets the difficult challenge of having a single antenna structure for matching the 50-Ω impedance of a rigid 2.2-mm-diameter coaxial structure to the impedance of cancerous tissue for effective tumor ablation, enabling *in situ* biological tissue type/state measurements to be made, and to allow biopsy samples to be extracted from (or to allow material to be introduced into) the human body without causing an adverse change in the EM field produced by the structure when used in ablation and measurement modes.

The multi-functional antenna structure supports the propagation of microwave energy at 14.5 GHz. The impedance of the structure has been matched to the impedance of the cancerous tissue to minimize losses and heating in the cable when full treatment power is being used. This structure also meets the challenge of introducing a biopsy tube (or needle) into the antenna, which involved developing a means of passing the biopsy sample (or other material) from the inner conductor to the outside of the coaxial structure without causing loss of function in terms of treatment and measurement capability. This was a difficult challenge because the biopsy material exhibits a high dielectric loss at such high microwave frequencies and also the high dielectric constant associated with the tissue disrupts the normal operation of the antenna.

In the final design, the connection to the biopsy tube (or center conductor) from the outside of the antenna structure was made using four 0.2-mm-diameter holes passing through the inner and outer conductor walls and through the intervening dielectric material. The presence of biopsy sample material in this short section of line was found to result in a small, but acceptable, reduction in the performance of the overall antenna structure.

The overall length of the final antenna structure was 120 mm from the tip of the ceramic radiator to the back end of the connector used to join the structure to a larger diameter flexible low-loss interface cable used to transport measurement and treatment energy between the antenna and the microwave instrumentation. 120 mm was chosen, as it allows access to the majority of tumors within the human breast or liver, which are the primary organs for which the system was developed to treat. It was also necessary to limit the length of the small diameter rigid coaxial structure as much as possible due to the increased insertion loss compared to that of the larger diameter interface cable. The OD of the final structure was 2.2 mm to ensure a minimal amount of scarring is caused when the structure is used to treat breast tumors and to help enable the shaft to be inserted directly into the breast. The outer jacket of the coaxial cable was made from stainless steel to prevent it bending when inserted percutaneously into various biological tissue structures. The inner surface of the outer conductor and the outer surface of the inner conductor were silver plated, and the dielectric material between the two conductors was a low-density PTFE with as much air as possible to minimize power loss within the structure. The ceramic radiator was made from a hard low-loss microwave ceramic material, which acts as an impedance transformer to match the 50-Ω impedance of the coaxial structure to the impedance of tumor, and also the geometry of the ceramic radiator was optimized, using CST Microwave Studio, to produce the desired near-field energy distribution into certain biological tissue structures. The hard ceramic material also enabled a tip to be designed and produced that was sharp enough to allow the structure to be inserted percutaneously without the need for an introducer.

The ablation feature has been demonstrated using *in vivo* and *in vitro* healthy tissue models and excised liver and breast tumors. The structure has also been used to demonstrate its ability to differentiate between a number of different *in vitro* tissue types and between healthy tissue and tumor in excised sections of human breast tissue.

The multi-functional antenna structure described in this paper has now been used with the dynamic impedance matching and near-field measurement system to successfully perform a number of pre-clinical and initial pilot clinical trials. The ability to repeatedly produce controlled spheres of ablation of up to 2.5 cm in diameter in healthy tissue and in excised tumors has been successfully tested, together with the ability to differentiate between healthy and cancerous tissue using excised liver and breast tumors. All results to date have been extremely positive. Ablation diameters of up to 38.8 mm $+/-$ 1.3 mm have been consistently produced in *ex-vivo* liver tumors using the antenna structure reported in this paper. The results from these clinical trials have now been presented at international medical conferences, and the tissue ablation work has been published in *The International Journal of Hyperthermia* [39].

ACKNOWLEDGMENT

The authors would like to thank the following people for their help and support during the development of the antenna and the overall tumor treatment and measurement system: Dr. M. Booton, S. Morris, Dr. J. Bishop, Dr. S. Chaudhry, Prof. I. Darwazeh, Dr. R. Sloan, Dr. P. Wall, and Dr. C. Duff. The authors would also like to thank MDi Limited for believing in the three original inventors of the new microwave breast tumor treatment and measurement system and for placing contracts with MicroOncology Ltd. to enable the overall system to be developed (the IP relating to the dynamic tissue matching, near-field tissue type/state measurement, bespoke method of calibration, and the dual-function antennas is owned by MDi Limited). The IP relating to the multi-functional antenna is owned by Creo Medical Limited.

REFERENCES

[1] J. W. Moorman, M. E. Bush, and A. M. Goodman, "Needle kit and method for microwave ablation, track coagulation and biopsy," U.S. Patent Appl. 2003/0195500, Oct. 16, 2003.

[2] A. Rosen, M. A. Stuchley, and A. V. Vorst, "Applications of RF/microwaves in medicine," *IEEE Trans. Microw. Theory Techn.*, vol. 50, no. 3, pp. 963–974, Mar. 2002.

[3] P. Cresson, C. Ricard, N. Bernardin, L. Dubois, and J. Pribetich, "Design and modeling of a specific microwave applicator for the treatment of snoring," *IEEE Trans. Microw. Theory Techn.*, vol. 54, no. 1, pp. 302–308, Jan. 2006.

[4] Z. Gu, C. M. Rappaport, P. J. Wang, and B. A. VanderBrink, "Development and experimental verification of the wide-aperture catheter-based microwave cardiac ablation antenna," *IEEE Trans. Microw. Theory Techn.*, vol. 48, no. 11, pp. 1892–1900, Nov. 2006.

[5] D. Despretz, J. C. Camart, C. Michel, J-J. Fabre, B. Prevost, J-P. Sozanski, and M. Chive, "Microwave prostatic hypothermia: Interest of urethral and rectal applicators combination—Theoretical study and animal experimental results," *IEEE Trans. Microw. Theory Techn.*, vol. 44, no. 10, pp. 1762–1768, Oct. 1996.

[6] K. Saito, Y. Hayashi, H. Yoshimura, and K. Ito, "Heating characteristics of array applicator composed of two coaxial-slot antennas for microwave coagulation therapy," *IEEE Trans. Microw. Theory Techn.*, vol. 48, no. 11, pp. 1800–1806, Nov. 2000.
[7] R. D. Nevels, G. D. Arndt, G. W. Raffoul, J. R. Carl, and A. Pacifico, "Microwave catheter design," *IEEE Trans. Biomed. Eng.*, vol. 45, no. 7, pp. 885–890, Jul. 1998.
[8] K. Saito, H. Yoshimura, K. Ito, Y. Aoyagi, and H. Horita, "Clinical trials of interstitial microwave hyperthermia by use of coaxial-slot antenna with two slots," *IEEE Trans. Microw. Theory Techn.*, vol. 52, no. 8, pp. 1987–1991, Aug. 2004.
[9] M. F. Iskander and A. M. Tumeh, "Design optimization of interstitial antennas," *IEEE Trans. Biomed. Eng.*, vol. 36, no. 2, pp. 238–245, Feb. 1989.
[10] C. P. Hancock, S. M. Chaudhry, and A. M. Goodman, "coaxial tissue ablation probe and method of making balun therefor," Eur. Patent EP1726268 (A1), Sep. 07, 2005.
[11] M. Lazebnik, L. McCartney, D. Popovic, C. B. Watkins, M. J. Lindstrom, J. Harter, S. Sewall, A. Magliocco, J. H. Booske, M. Okoniewski, and S. C. Hagness, "A large-scale study of the ultrawideband microwave dielectric properties of normal breast tissue obtained from reduction surgeries," *Phys. Med. Biol.*, vol. 52, pp. 2637–2656, 2007.
[12] J. P. Grant, R. N. Clarke, G. T. Symm, and N. M. Spyrou, "*In vivo* dielectric properties of human skin from 50 MHz to 2.0 GHz," *Phys. Med. Biol.*, vol. 33, no. 5, pp. 607–612, 1988.
[13] D. Misra, M. Chabbra, B. R. Epstein, M. Mirotznik, and K. R. Foster, "Noninvasive electrical characterization of materials at microwave frequencies using an open-ended coaxial line: Test of an improved calibration technique," *IEEE Trans. Microw. Theory Techn.*, vol. 38, no. 1, pp. 8–13, Jan. 1990.
[14] A. Nyshadham, C. L. Sibbald, and S. S. Stuchly, "Permittivity measurements using open-ended sensors and reference liquid calibration—An uncertainty analysis," *IEEE Trans. Microw. Theory Techn.*, vol. 40, no. 2, pp. 305–313, Feb. 1992.
[15] D. Berube, F. M. Ghannouchi, and P. Savard, "A comparative study of four open-ended coaxial probe models for permittivity measurements of lossy dielectric/biological materials at microwave frequencies," *IEEE Trans. Microw. Theory Techn.*, vol. 44, no. 10, pp. 1928–11933, Oct. 1996.
[16] C. P. Hancock and J. Bishop, "Tissue detection and ablation apparatus and method of actuating a tuner," Eur. Patent EP1748726 (A1), Feb. 07, 2007.
[17] C. P. Hancock and J. Bishop, "Tissue detection and ablation apparatus and method of actuating a tuner," US Patent US2008234574 (A1), Sep. 25, 2008.
[18] C. P. Hancock, S. M. Chaudhry, P. Wall, and A. M. Goodman, "Proof of concept percutaneous treatment system to enable fast and finely controlled ablation of biological tissue," *Med. Biol. Eng. Comput.*, vol. 45, no. 6, pp. 531–540, Jun. 2007.
[19] A. S. Wright, L. A. Sampson, T. F. Warner, D. M. Mahvi, and F. T. Lee, "Radiofrequency versus microwave ablation in hepatic porcine model," *Radiology*, vol. 236, no. 1, pp. 132–139, 2005.
[20] A. D. Strickland, P. J. Clegg, N. J. Cronin, B. Swift, M. Festing, K. P. West, G. S. M. Robertson, and D. M. Lloyd, "Experimental study of large-volume microwave ablation in the liver," *Br. J. Surgery*, vol. 89, pp. 1003–1007, 2002.
[21] A. S. Wright, F. T. Lee, Jr., and D. M. Mahvi, "Hepatic microwave ablation with multiple antennae results in synergistically larger zones of coagulation necrosis," *Ann. Surg. Oncol.*, vol. 10, pp. 275–283, 2003.
[22] M. S. Metcalfe, F. H. G. Bridgewater, E. Mullin, and G. J. Maddern, "Useless and dangerous—Fine needle aspiration of hepatic colorectal metastases," *Br. Med. J.*, vol. 328, pp. 507–508, Feb. 2004.
[23] "How breast cancer is diagnosed" Macmillian Cancer Support, 2012. [Online]. Available: http://www.macmillan.org.uk/Cancerinformation/Cancertypes/Breast/Symptomsdiagnosis/Diagnosis.aspx#FNA
[24] C. P. Hancock, "Pushing forward new frontiers in microwave and millimetre wave medical treatment systems," in *IEEE Asia–Pacific Microw. Conf.*, Dec. 2007, Tutorial, Session 5A.
[25] C. P. Hancock, S. M. Chaudhry, and A. M. Goodman, "Tissue ablation apparatus," Eur. Patent EP1569570 (A2), Sep. 07, 2005.
[26] C. P. Hancock, S. M. Chaudhry, and A. M. Goodman, "Tissue ablation apparatus and method of ablating tissue," U.S. Patent US2006155270 (A1), Jul. 13, 2006.
[27] C. P. Hancock, M. White, J. Bishop, and M. W. Booton, "Apparatus for treating tissue with microwave radiation and antenna calibration system and method," Eur. Patent EP2069014 (A2), Jun. 17, 2009.
[28] C. P. Hancock, M. White, J. Bishop, and M. W. Booton, "Apparatus for treating tissue with microwave radiation and antenna calibration system and method," Chinese Patent CN101583398 (A), Nov. 18, 2009.
[29] C. P. Hancock, J. Bishop, and M. W. Booton, "Tissue classifying apparatus," U.S. Patent Appl. US2010168730 (A1), Jul. 01, 2010.
[30] C. P. Hancock, J. Bishop, and M. W. Booton, "Tissue classifying apparatus," Eur. Patent Appl. EP117456 (A2), Nov. 18, 2009.
[31] C. P. Hancock, J. Bishop, and M. W. Booton, "Tissue classifying apparatus," Can. Patent Appl. CA2714268 (A1), Sep. 18, 2008.
[32] K. Jung-Mu, O. Donghoon, Y. Jeonghoon, C. Sungjoon, C. Jeiwan, K. Youngwoo, C. Changyul, and K. Yong-Kweon, "*in vitro* and *in vivo* measurements for biological applications using micromachined probe," *IEEE Trans. Microw. Theory Techn.*, vol. 53, no. 11, pp. 3415–3421, Nov. 2005.
[33] "Electrical characteristics of biological tissue over a wide range of frequencies," IFAC, Florence, Italy, 1997–2010. [Online]. Available: http://niremf.ifac.cnr.it/tissprop
[34] C. P. Hancock and M. White, "Tissue measurement and ablation antenna," U.S. Patent Appl. US2010228244 (A1), Sep. 09, 2009.
[35] C. P. Hancock and M. White, "Tissue measurement and ablation antenna," Eur. Patent EP2120763 (A1), Nov. 25, 2009.
[36] C. P. Hancock, "Needle structure and method of performing needle biopsies," U.S. Patent Appl. US2010030107 (A1), Feb. 04, 2010.
[37] C. P. Hancock, "Needle structure and method of performing needle biopsies," Can. Patent Appl. CA2701957 (A1), Apr. 17, 2008.
[38] A. Chaudhry, B. Baruah, A. Goyal, T. Kink, P. Young, A. Douglas-Jones, and R. Mansel, "Differences in dielectric properties between malignant and normal breast tissue: Preliminary results of the microblate study," in *32nd Annu. CTRC–AACR Breast Cancer Symp.*, San Antonio, TX, USA, Dec. 10–13, , 2009.
[39] R. P. Jones, N. R. Kitteringham, M. Terlizzo, C. P. Hancock, D. Dunne, S. W. Fenwick, G. J. Poston, P. Ghaneh, and H. Z. Malik, "Microwave ablation of *ex vivo* human liver and colorectal liver metastases," *Int. J. Hyperthermia*, vol. 28, no. 1, pp. 43–54, Feb. 2012.
[40] S. M. Chaudhry and C. P. Hancock, "Microwave tumour ablation—Breast cancer treatment system—User requirements specification," MicroOncol. Ltd. (for MDi Limited), Chepstow, South Wales, U.K., MB2_URS002_4_0_UserReqSpec, Internal Doc., Sep. 2007.

Chris P. Hancock (SM'07) received the Ph.D. degree in electronic engineering from Bangor University, Bangor, U.K., in 1996.

From 1997 to 2002, he was a Senior Microwave Engineer with Gyrus Medical Ltd. In 2003, he founded MicroOnclogy Ltd. (now Creo Medical Limited), Chepstow, U.K., to develop his ideas based on dynamic impedance-matching techniques and integrated RADAR measurement techniques using Ku-band energy for the treatment of breast tumors. In 2009, he was given a personal Chair with the Medical Microwave Systems Research Group, Bangor University. He is also the Chief Technical Officer (CTO) and founder of Creo Medical Limited.

Prof. Hancock is a Chartered Engineer and a Chartered Physicist. He is a Fellow of the Institution of Engineering and Technology (IET) and the Institute of Physics. He was the recipient of an Honorary Research Fellowship at University College London for his work on breast cancer treatment.

Nuwan Dharmasiri received the Masters degree from Kings College London, London, U.K., in 2000, and the Ph.D. degree from the University of Manchester, Manchester, U.K., in 2006.

In 2007, he joined the Research and Develooment Group, Creo Medical Limited (formerly MicroOncology Ltd.), where he was involved with microwave measurement and calibration techniques for their system. In 2008/2009, his research focused on developing systems combining low-frequency RF and microwave energy. In 2010, he joined the Product Development Team to develop the CRoMa system that comprises bipolar RF and microwave.

Malcolm White received an Honours degree in physics from Exeter University, Exeter, U.K., in 1977.

From 1977 to 1983, he was with the Microwave Tube Division, MO Valve Company [part of GEC (UK)], where he developed miniature magnetrons with small magnetic circuits. From 1983 to 2012, he was with the Radar Cross Section (RCS) Department, Thales UK, as a Microwave Engineer, Trials Engineer, and Mathematical Engineer involved with most aspects of RCS measurement, prediction, analysis, and software design (FACETS RCS prediction software), as well as radar, antenna, filter, and signal processing design. For several years, he was Co-Presenter of The RCS Course and The FACETS Training Course to delegates from industry and government agencies. Since 2012, he has been with Creo Medical Limited, Chepstow, U.K., where he has been involved in the design and development of novel medical tools using microwaves.

Mr. White is a Chartered Physicist. He is a member of the Institute of Physics and the Institution of Engineering and Technology (IET).

Andrew M. Goodman was born in Luton, U.K., in 1972. He received the B.Eng., M.Sc., and Ph.D. degrees from Bangor University, Bangor, U.K., in 1993, 1996, and 1999, respectively, and the M.A. degree from the Royal College of Art, London, U.K., in 2008.

From 2000 to 2004, he was with Nakamura Laboratory, Tohoku University, Sendai, Japan, where he investigated magnetization reversal mechanisms in perpendicular magnetic recording media. Since 2011, he has been Director of the Design Studio, Pontio, a center for arts and design innovation. His research interests are focused on methodology and practice in interdisciplinary design-led innovation.

Dr. Goodman was the recipient of a 2000 European Union (EU) Research Fellowship to Japan.